

Brief Description

The ANL suite of fast reactor analysis codes was used to analyze the RBEC benchmark problem. Detailed fuel cycle analysis was performed using the DIF3D/REBUS-3 code system. Multi-group cross section data was generated for each homogenized zone in the benchmark using the MC²-2 code based upon ENDF/B-V.2 data. The flux calculations were performed using the discrete ordinate transport code TWODANT with comparative results generated using the DIF3D finite difference diffusion theory option (DIF3D-FD).

For each of the 15 homogenized physical zones, 33-group and 230-group cross section structures were implemented for the specified composition and component-wise temperatures using the MC²-2 code. ENDF/B-V.2 data was used for all isotopes. For the three core zones, a critical buckling calculation was used with a consistent P₁ approximation and the corresponding spectrum was used for group collapsing. For the remaining compositions, a fixed source, derived from the leakage spectrum from an adjacent zone, was used to determine the collapsing spectrum. As an example, the leakage spectrum from the core zone were used as a fixed source in the adjoining blanket region to obtain a new collapsing spectrum. The leakage spectrum derived from the blanket calculation was then used as a fixed source in the fission gas plenum. This process is replicated for all other regions progressing the leakage from the core through all adjoining regions in the domain.

For resolved resonance integral calculation, the narrow resonance approximation was used, and the Doppler broadening, interference scattering, and the effects of overlap with neighboring resolved resonances were taken into account. It is noteworthy that an additional option is available to use the hyper-fine group integral transport calculation with RABANL, in which the Doppler width is divided into a few hyper-fine groups. In the preparation of MC²-2 library, wide and extremely weak resonances are pre-processed and represented by the ultra-fine-group (2082 group) energy structure of MC²-2. The other resonances are modeled by their resonance parameters, and their self-shielding effects are explicitly evaluated in the MC²-2 calculation. The unresolved resonance integral calculation was performed with a narrow resonance approximation, and interference scattering, the effects of overlap with resonances in other spin sequences, and the effects of self-overlap with resonances of the same spin sequences were taken into account. The resolved and unresolved energy range used is specified by the ENDF data and is unique for each nuclide. The (n,2n) reaction was treated as a source term in the ultra-fine-group spectrum calculation. For the secondary energy distribution, tabulated function, evaporation spectrum and discrete levels were used. The discrete ultra-fine-group (n,2n) scattering source was approximately treated by neglecting the energy-angle correlation.

The flux distributions are derived from the TWODANT transport theory code using the 33-group cross section set unless otherwise specified. An R-Z computational model was employed in these calculations with ~2.0 cm mesh size. For comparison, the finite difference diffusion theory option of the DIF3D was also used. It is noted that the DIF3D code is a collection of modules that provide various solution options for eigenvalue and fixed source problems: variational nodal transport (VARIANT), nodal diffusion theory, and finite difference diffusion theory options. The power distributions were not obtained along the discrete lines specified but instead derived from mesh centered quantities. As an example, the first radial mesh was 2.39 cm wide. The power was calculated for the series of meshes from the bottom of the core to the top within this first mesh and thus belongs to the volume associated with a 2.39 cm wide strip. A similar approach was taken for the radial power distributions where the mesh size was 2.5 cm in both cases.

The fuel cycle analyses were performed using the REBUS-3 code, which was developed for fast reactor depletion and fuel cycle analysis. Both the core and blanket zones were represented by five axial depletion regions. The region density iteration was performed with a relative convergence criterion of 0.0005 on calculated material densities. That is, the depletion calculation for each region was performed with the average of the beginning and end of time interval fluxes. The end of time interval flux was iteratively computed by iteration on the final nuclide densities. The depletion calculations were performed using burnup chains for nuclides ranging from U-234 to Cm-246. Capture, (n,2n), and fission reactions were considered for all actinide isotopes included in the burn chains. In the capture and (n,2n) reactions, short-lived intermediate products were neglected. As a result, the products of capture reactions of U-238, Np-238, Pu-242, and Am-243 were

represented by Pu-239, Pu-239, Am-243, and Cm-244, respectively. The capture reaction of Am-241 was modeled to yield Cm-242, Am-242m, and Pu-242 with yield fractions of 0.66, 0.20, and 0.14, respectively. The products of (n,2n) reactions of Pu-238 and Am-241 were respectively represented by N-237 and Pu-240. The (n,2n) reaction of Am-243 was assumed to yield Am-242m, Pu-242, and Cm-242 with yield fractions of 0.5, 0.086, and 0.414, respectively. Cm-242 was assumed to yield Am-241 in 99% of its (n,2n) reactions and Np-237 in 1%. It was assumed that 37.4% of (n,2n) reactions of Np-237 yield U-236 and the remaining 62.6% yield a fictitious dummy isotope. The end products of Cm-246 capture and U-234 (n,2n) reactions were represented by a fictitious dummy isotope. Important α and β decays of actinide isotopes were also considered. Specifically, α decay was considered for all actinide isotopes except for Np-238 and Pu-241. The β^- decays of Np-238, Pu-241, Am-242m and the β^+ decay of Am-242m were also included in the burn chains. The employed decay constants for the β^- , β^+ , and α decays of Am-242m were 1.189E-10, 2.487E-11, and 7.225E-13, respectively. The fission products were modeled with five lumped rare earth elements and five lumped fission products. The cross sections of these lumped elements were generated by weighting the cross sections of 180 fission products with fission yields of U-235, U-238, Pu-239, Pu-240, and Pu-241, respectively. Three dummy isotopes were also used to represent the other end products not included in the chains. For full reactor depletion calculations, the lumped fission products of U-234, U-235, and U-236 were represent by those of U-235, while the fission products of U-237, U-238, Np-237, Np-238, and Pu-238 were represented by those of FP38. The fission products of Pu-241 and higher actinides were represented by those of Pu-241.

A 100-day depletion time interval was used for all calculations. For Mode 3, two options of the REBUS-3 module were used. The first follows the approach described in the benchmark where 1/6 of the core material is replaced with fresh fuel during each shutdown phase. That is, 1/6 of each of once-burned to six-cycle-burned fuels is replaced with fresh fuel. The second utilizes the equilibrium cycle option of REBUS-3 where the six-cycle burned fuel is replaced with fresh fuel. In Figure 3.A, the eigenvalue results of the two approaches are merged where the equilibrium cycle calculation are represented as horizontal lines. As seen, at the sixth cycle, the Mode 3 calculation is quite different from that predicted by the equilibrium cycle calculation. It is important to note that if one continues the approach used in Mode 3 for additional fuel cycles that the solution will degrade further. This is due to the fact that there will be fuel material in the core for more than six cycles in the Mode 3 approach which is not the case for the equilibrium cycle option.

Number of energy group: 33 and 230

Use codes: MC²-2 and REBUS-3 (with TWODANT and DIF3D)

Use nuclear data set: ENDFB-V.2

Table. 1.1 BOC k_{eff} value from different codes

BOC k_{eff}	
Codes	k_{eff} value
DIF3D-FD	0.99721
TWODANT S8	0.99848

Table. 1.2 k_{eff} by time step (Mode.1)

day	k_{eff} for 900MW, 1800 Days Cycle			
	Codes			
	REBUS-3 DIF3D-FD 33 group	REBUS-3 TWODANT 33 group	REBUS-3 DIF3D-FD 230group	REBUS-3 TWODANT 230group
0	0.99721	0.99848	0.99781	0.99937
200	1.00058	1.00183	1.00118	1.00269
400	1.00322	1.00446	1.00383	1.00530
600	1.00517	1.00643	1.00579	1.00725
800	1.00649	1.00777	1.00712	1.00858
1000	1.00723	1.00854	1.00787	1.00935
1200	1.00745	1.00881	1.00810	1.00962
1400	1.00721	1.00861	1.00788	1.00943
1600	1.00657	1.00802	1.00725	1.00884
1800	1.00557	1.00708	1.00626	1.00791

Table. 1.3 Region powers and power peaking factors (Mode.1)

Mode.1					
	ZONE	Power(Watts)	Power Density (Watts/cc)	Peak Density (Watts/cc)	Peak to AVG. Power Density
BOC	Core1	331443000	142	189	1.3
	Core2	397293000	127	194	1.5
	Core3	150081000	101	159	1.6
EOC	Core1	312449000	134	172	1.3
	Core2	370533000	118	174	1.5
	Core3	143851000	97	144	1.5

Table. 1.4 Volume averaged neutron spectra in the core (Mode.1)

Mode.1						
day	BOC			EOC		
Upper group bound. Energy	Core.1	Core.2	Core.3	Core.1	Core.2	Core.3
1.4191E+07	4.9722E+17	5.8139E+17	1.9870E+17	4.6697E+17	5.3960E+17	1.9243E+17
1.0000E+07	8.7784E+18	1.0275E+19	3.4483E+18	8.2440E+18	9.5355E+18	3.3407E+18
6.0653E+06	4.2280E+19	4.9255E+19	1.6202E+19	3.9673E+19	4.5673E+19	1.5697E+19
3.6788E+06	1.1531E+20	1.2934E+20	4.0681E+19	1.0867E+20	1.2040E+20	3.9591E+19
2.2500E+06	2.3804E+20	2.5591E+20	7.2074E+19	2.2731E+20	2.4097E+20	7.0947E+19
1.3647E+06	3.9964E+20	4.2020E+20	1.2007E+20	3.8017E+20	3.9528E+20	1.1836E+20
8.3465E+05	6.6113E+20	6.8701E+20	2.0207E+20	6.2076E+20	6.4145E+20	1.9836E+20
5.1047E+05	8.0049E+20	8.2729E+20	2.4239E+20	7.5236E+20	7.7465E+20	2.3861E+20
3.0962E+05	8.1538E+20	8.3207E+20	2.4038E+20	7.7177E+20	7.8477E+20	2.3770E+20
1.8779E+05	7.3310E+20	7.4429E+20	2.0807E+20	6.9438E+20	7.0327E+20	2.0579E+20
1.1486E+05	5.9962E+20	6.0734E+20	1.6471E+20	5.6418E+20	5.7152E+20	1.6214E+20
6.9663E+04	5.8997E+20	5.8759E+20	1.6118E+20	5.5056E+20	5.5006E+20	1.5748E+20
4.2253E+04	3.6205E+20	3.5781E+20	8.8467E+19	3.3559E+20	3.3333E+20	8.6022E+19
2.5842E+04	4.3618E+20	4.1837E+20	1.0770E+20	4.0091E+20	3.8765E+20	1.0378E+20
1.5674E+04	2.6183E+20	2.4266E+20	5.1821E+19	2.3820E+20	2.2315E+20	4.9559E+19
9.5864E+03	1.4266E+20	1.2824E+20	2.3858E+19	1.2834E+20	1.1695E+20	2.2635E+19
5.8631E+03	1.1760E+20	1.0291E+20	1.9717E+19	1.0372E+20	9.2424E+19	1.8373E+19
3.5561E+03	6.8062E+19	5.7474E+19	9.9598E+18	5.8677E+19	5.0704E+19	9.1002E+18
2.1569E+03	3.7400E+19	3.0190E+19	5.1210E+18	3.1257E+19	2.5993E+19	4.5495E+18
1.3192E+03	1.5593E+19	1.2151E+19	1.9220E+18	1.2671E+19	1.0225E+19	1.6576E+18
8.0012E+02	7.5634E+18	5.8392E+18	9.8114E+17	5.6801E+18	4.6048E+18	7.7923E+17
4.8530E+02	2.1615E+18	1.6253E+18	3.1231E+17	1.5150E+18	1.2128E+18	2.3388E+17
3.2803E+02	1.2905E+18	9.4879E+17	2.5600E+17	7.6361E+17	6.1562E+17	1.6073E+17
1.6020E+02	1.9349E+17	1.4052E+17	6.6979E+16	8.8689E+16	7.3815E+16	3.4861E+16
9.9627E+01	4.7173E+16	3.5085E+16	2.3569E+16	1.5077E+16	1.3526E+16	9.0324E+15
7.4423E+01	3.5575E+16	2.7363E+16	2.3685E+16	7.6996E+15	7.5676E+15	6.7329E+15
4.4025E+01	1.2393E+16	9.8496E+15	9.2105E+15	2.8780E+15	2.9102E+15	2.7106E+15
2.4981E+01	2.2155E+15	1.7496E+15	1.1151E+15	5.5221E+14	5.4586E+14	3.3118E+14
1.5278E+01	2.1584E+15	1.6960E+15	1.2186E+15	1.4199E+14	1.6313E+14	1.0899E+14
9.3443E+00	4.9126E+14	3.8512E+14	2.2241E+14	4.1410E+13	4.5727E+13	2.2643E+13
4.5257E+00	2.5921E+15	2.3023E+15	2.5873E+15	5.4091E+13	1.4100E+14	2.6954E+14
6.1248E-01	1.3947E+14	1.1680E+14	1.1720E+14	3.5947E+12	5.5065E+12	7.2214E+12
4.7304E-01	2.2800E+14	1.8428E+14	1.1391E+14	8.2885E+11	1.2535E+12	1.1543E+12

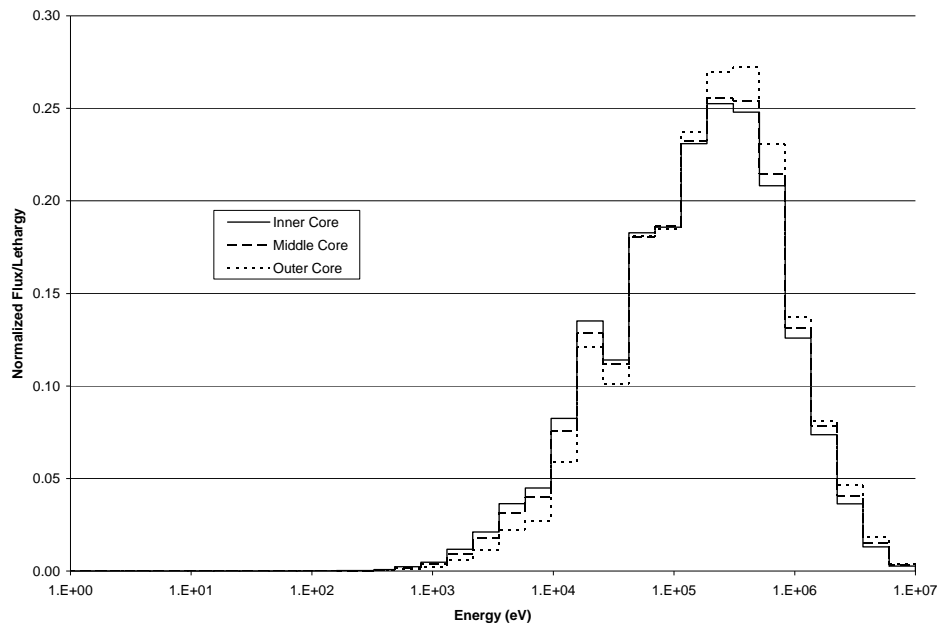


Figure 1.A. BOC Normalized Flux.

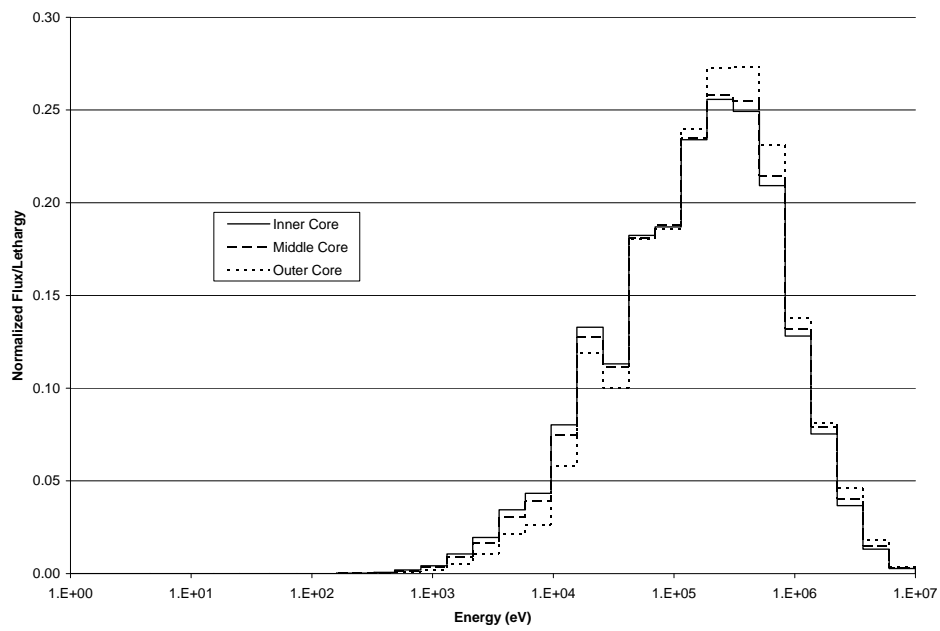


Figure 1.B. EOC Normalized Flux.

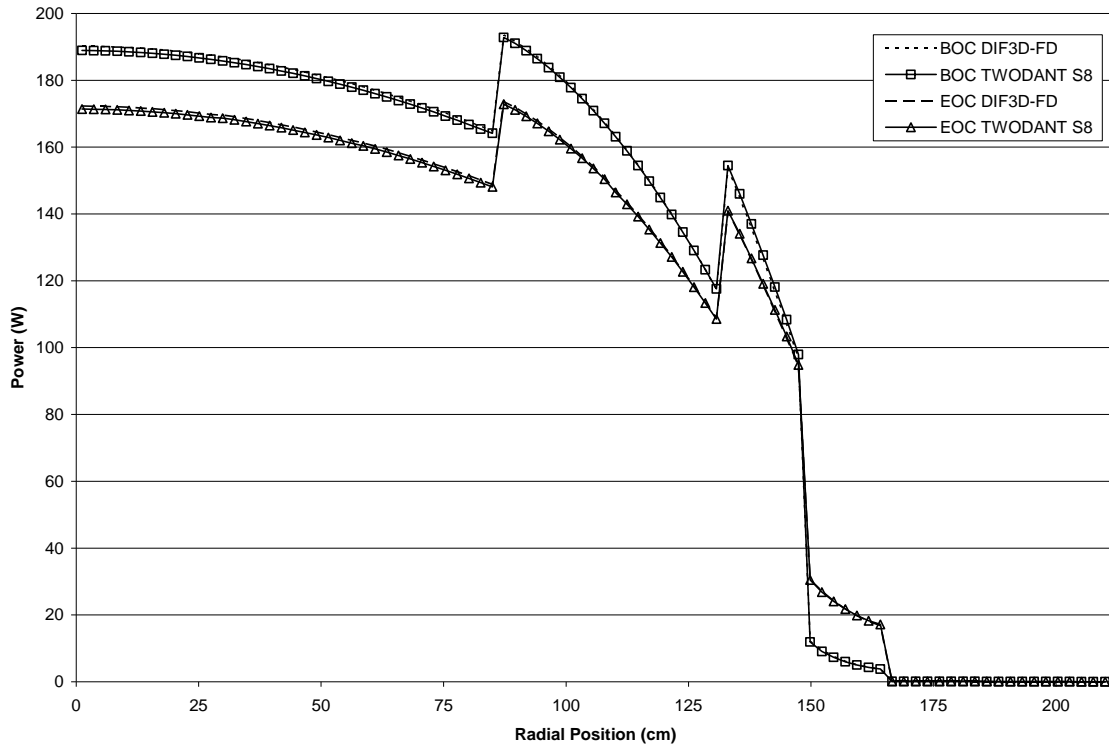


Figure 1.C. Radial Power Plot at Core Midplane.

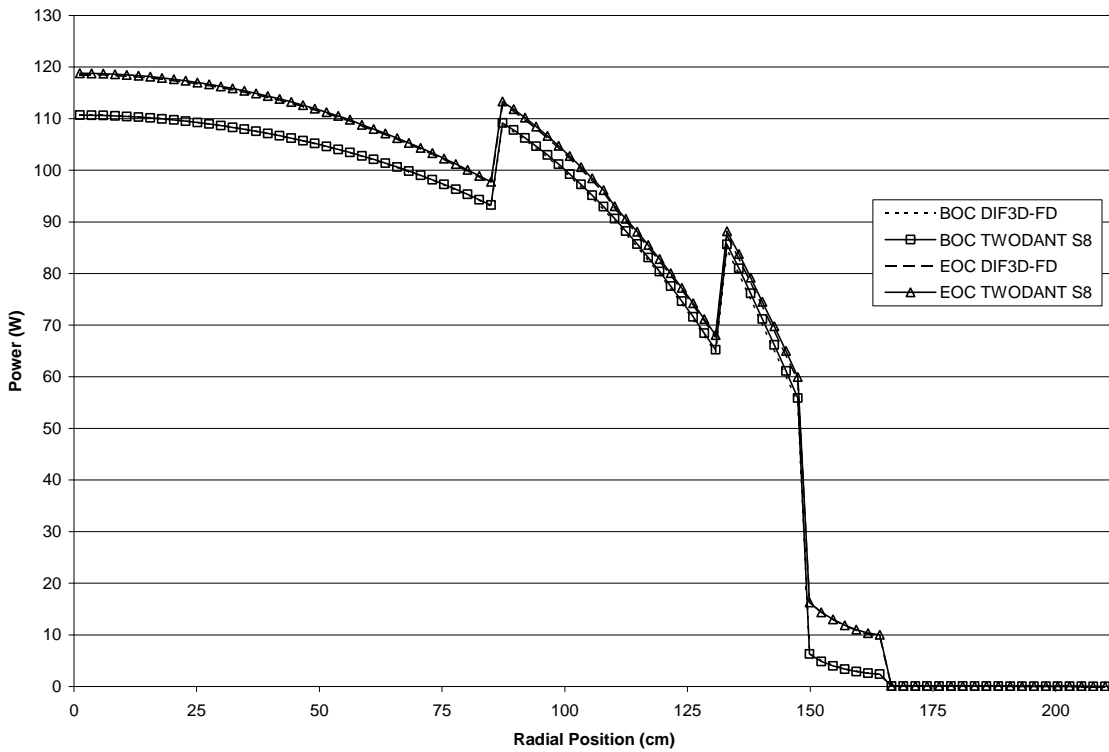


Figure 1.D. Radial Power Plot 45 cm above Core Midplane.

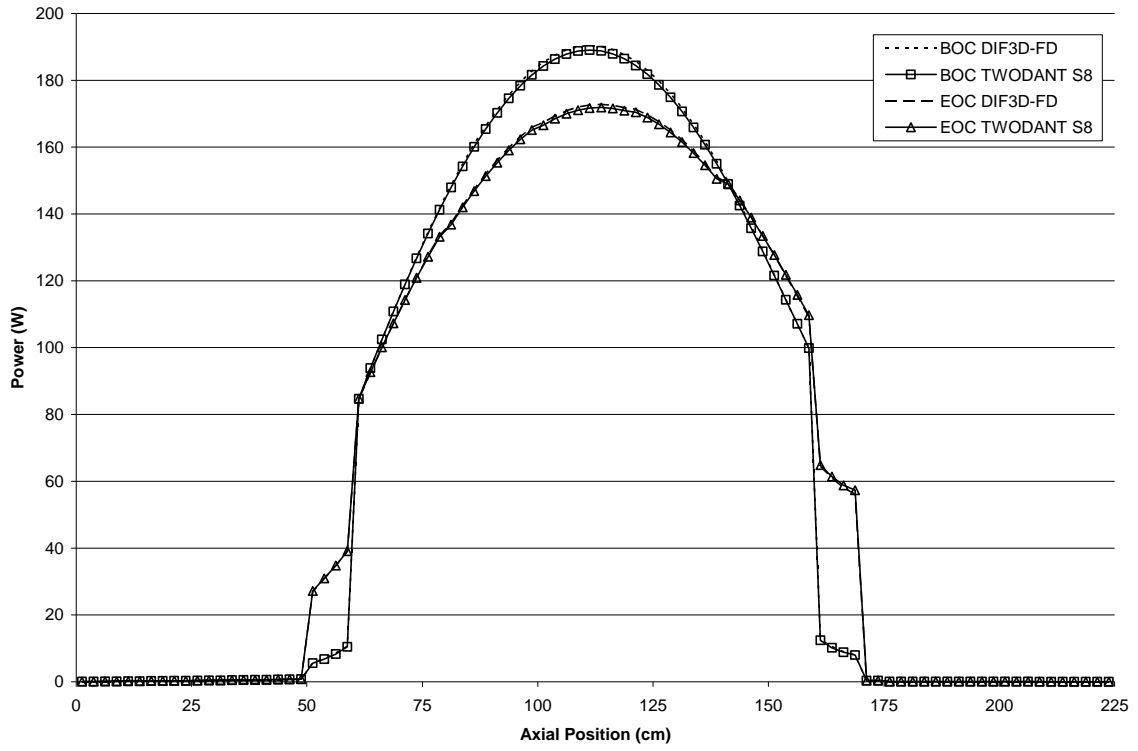


Figure 1.E. Axial Power Plot at Core Centerline.

Table. 2.2 keff by time step (Mode.2)

Mode.1				
k _{eff} for 900MW, 900 Days Cycle				
day	Codes			
	REBUS-3 DIF3D-FD 33 group	REBUS-3 TWODANT 33 group	REBUS-3 DIF3D-FD 230 group	REBUS-3 TWODANT 230 group
0	0.99721	0.99848	0.99781	0.99937
100	1.00058	1.00024	1.00118	1.00112
200	1.00199	1.00183	1.00260	1.00269
300	1.00322	1.00323	1.00383	1.00408
400	1.00428	1.00446	1.00490	1.00530
500	1.00517	1.00553	1.00579	1.00636
600	1.00591	1.00643	1.00653	1.00725
700	1.00649	1.00717	1.00712	1.00799
800	1.00693	1.00777	1.00756	1.00858
900	1.00740	1.00822	1.00787	1.00903

Table. 2.3 Region powers and power peaking factors (Mode.2)

Mode.2					
	ZONE	Power(Watts)	Power Density (Watts/cc)	Peak Density (Watts/cc)	Peak to AVG. Power Density
BOC	Core1	331443000	142	189	1.3
	Core2	397293000	127	194	1.5
	Core3	150081000	101	159	1.6
EOC	Core1	328905000	141	188	1.3
	Core2	379487000	121	184	1.5
	Core3	142678000	96	147	1.5

Table. 2.4 Volume averaged neutron spectra in the core (Mode.2)

Mode.1						
Upper group bound. Energy	BOC			EOC		
	Core.1	Core.2	Core.3	Core.1	Core.2	Core.3
1.4191E+07	4.9722E+17	5.8139E+17	1.9870E+17	4.9015E+17	5.5124E+17	1.8913E+17
1.0000E+07	8.7784E+18	1.0275E+19	3.4483E+18	8.6534E+18	9.7417E+18	3.2828E+18
6.0653E+06	4.2280E+19	4.9255E+19	1.6202E+19	4.1659E+19	4.6678E+19	1.5424E+19
3.6788E+06	1.1531E+20	1.2934E+20	4.0681E+19	1.1386E+20	1.2283E+20	3.8829E+19
2.2500E+06	2.3804E+20	2.5591E+20	7.2074E+19	2.3655E+20	2.4452E+20	6.9241E+19
1.3647E+06	3.9964E+20	4.2020E+20	1.2007E+20	3.9600E+20	4.0136E+20	1.1557E+20
8.3465E+05	6.6113E+20	6.8701E+20	2.0207E+20	6.5001E+20	6.5384E+20	1.9434E+20
5.1047E+05	8.0049E+20	8.2729E+20	2.4239E+20	7.8678E+20	7.8868E+20	2.3369E+20
3.0962E+05	8.1538E+20	8.3207E+20	2.4038E+20	8.0366E+20	7.9631E+20	2.3247E+20
1.8779E+05	7.3310E+20	7.4429E+20	2.0807E+20	7.2219E+20	7.1304E+20	2.0137E+20
1.1486E+05	5.9962E+20	6.0734E+20	1.6471E+20	5.8816E+20	5.8063E+20	1.5911E+20
6.9663E+04	5.8997E+20	5.8759E+20	1.6118E+20	5.7556E+20	5.6022E+20	1.5521E+20
4.2253E+04	3.6205E+20	3.5781E+20	8.8467E+19	3.5175E+20	3.4031E+20	8.5007E+19
2.5842E+04	4.3618E+20	4.1837E+20	1.0770E+20	4.2139E+20	3.9681E+20	1.0308E+20
1.5674E+04	2.6183E+20	2.4266E+20	5.1821E+19	2.5139E+20	2.2929E+20	4.9432E+19
9.5864E+03	1.4266E+20	1.2824E+20	2.3858E+19	1.3608E+20	1.2066E+20	2.2671E+19
5.8631E+03	1.1760E+20	1.0291E+20	1.9717E+19	1.1090E+20	9.6057E+19	1.8569E+19
3.5561E+03	6.8062E+19	5.7474E+19	9.9598E+18	6.3321E+19	5.3130E+19	9.2856E+18
2.1569E+03	3.7400E+19	3.0190E+19	5.1210E+18	3.4177E+19	2.7545E+19	4.7053E+18
1.3192E+03	1.5593E+19	1.2151E+19	1.9220E+18	1.4007E+19	1.0945E+19	1.7380E+18
8.0012E+02	7.5634E+18	5.8392E+18	9.8114E+17	6.4904E+18	5.0735E+18	8.4876E+17
4.8530E+02	2.1615E+18	1.6253E+18	3.1231E+17	1.7859E+18	1.3715E+18	2.6202E+17
3.2803E+02	1.2905E+18	9.4879E+17	2.5600E+17	9.6442E+17	7.3958E+17	1.9483E+17
1.6020E+02	1.9349E+17	1.4052E+17	6.6979E+16	1.2449E+17	9.7255E+16	4.6052E+16
9.9627E+01	4.7173E+16	3.5085E+16	2.3569E+16	2.4101E+16	2.0123E+16	1.3594E+16
7.4423E+01	3.5575E+16	2.7363E+16	2.3685E+16	1.4212E+16	1.2851E+16	1.1523E+16
4.4025E+01	1.2393E+16	9.8496E+15	9.2105E+15	5.2414E+15	4.8352E+15	4.5713E+15
2.4981E+01	2.2155E+15	1.7496E+15	1.1151E+15	9.5614E+14	8.7429E+14	5.5451E+14
1.5278E+01	2.1584E+15	1.6960E+15	1.2186E+15	3.7333E+14	3.9213E+14	2.8818E+14
9.3443E+00	4.9126E+14	3.8512E+14	2.2241E+14	9.9075E+13	9.9553E+13	5.4661E+13
4.5257E+00	2.5921E+15	2.3023E+15	2.5873E+15	4.2306E+14	6.5112E+14	9.7038E+14
6.1248E-01	1.3947E+14	1.1680E+14	1.1720E+14	1.6810E+13	2.2288E+13	2.8602E+13
4.7304E-01	2.2800E+14	1.8428E+14	1.1391E+14	4.8574E+12	7.4124E+12	7.1936E+12

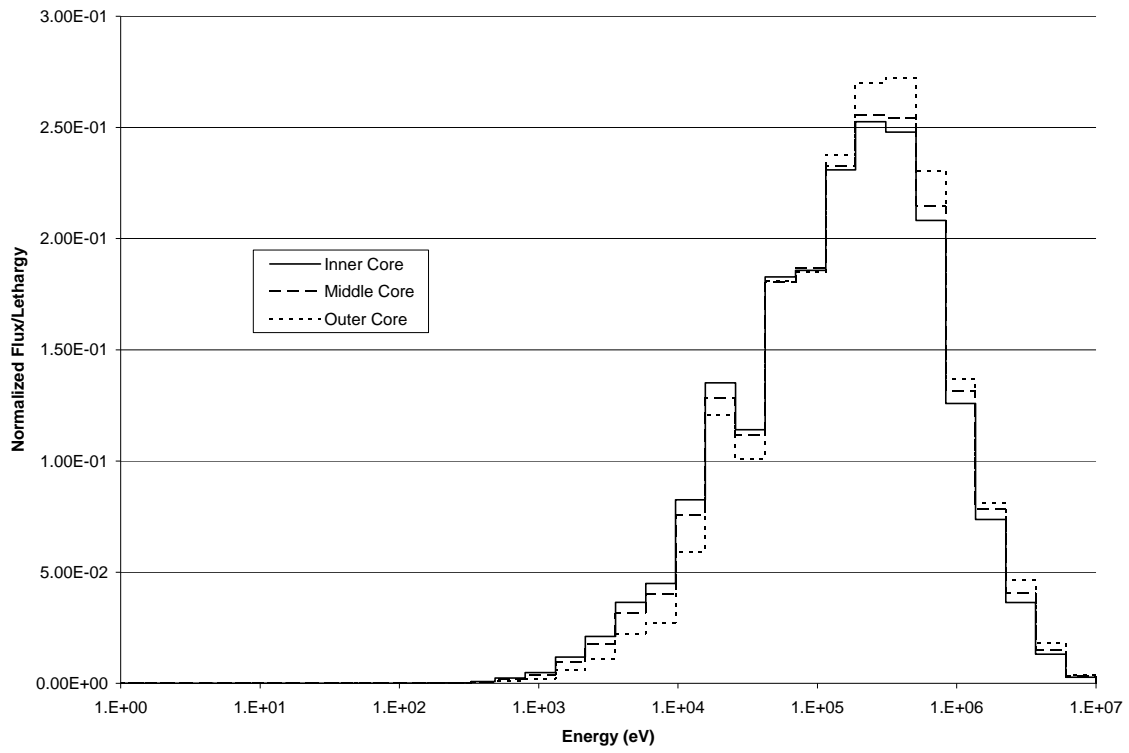


Figure 2.A. BOC Normalized Flux.

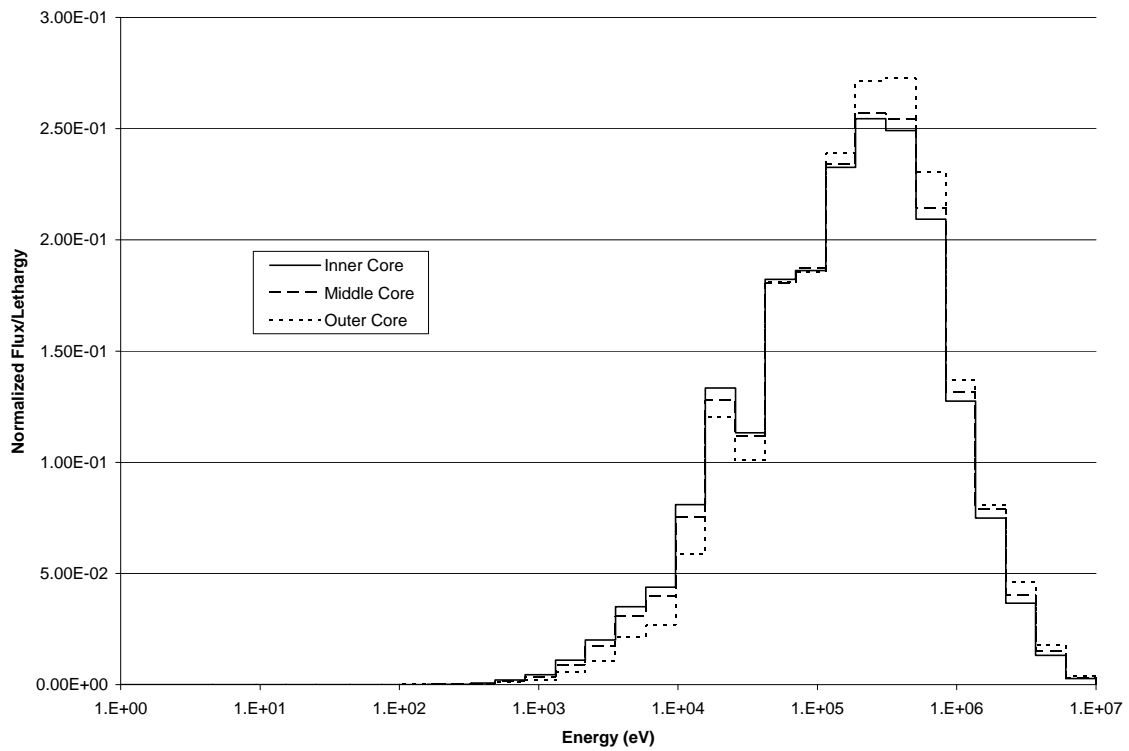


Figure 2.B. EOC Normalized Flux.

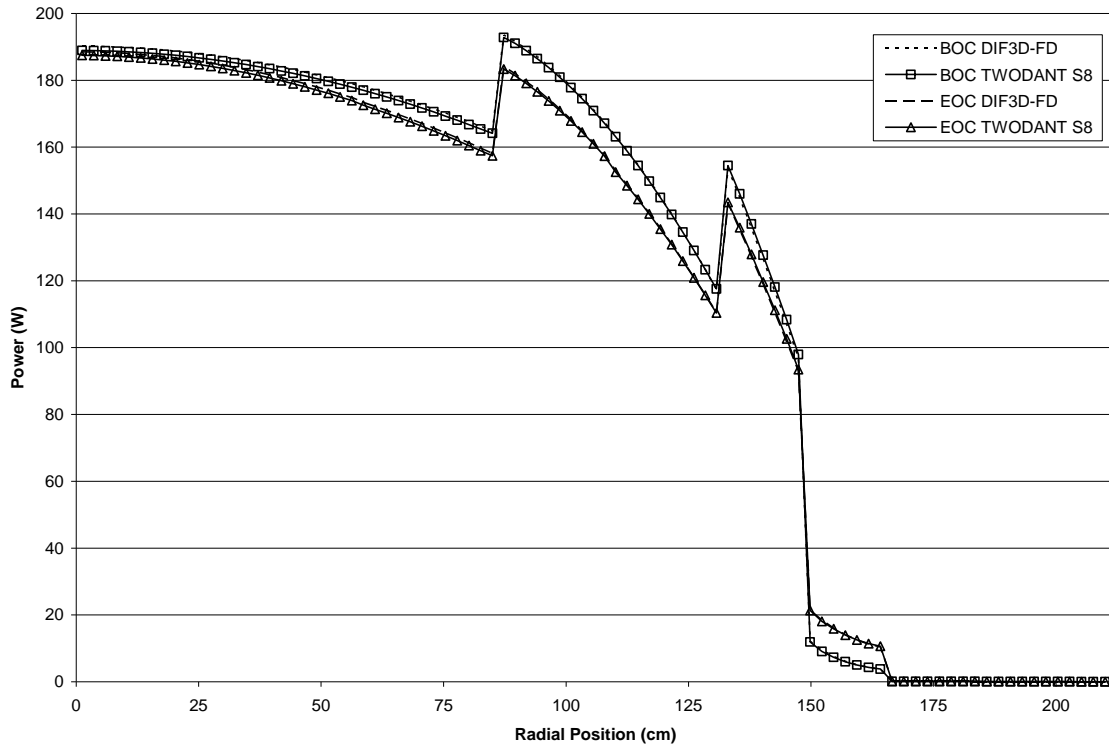


Figure 2.C. Radial Power Plot at Core Midplane.

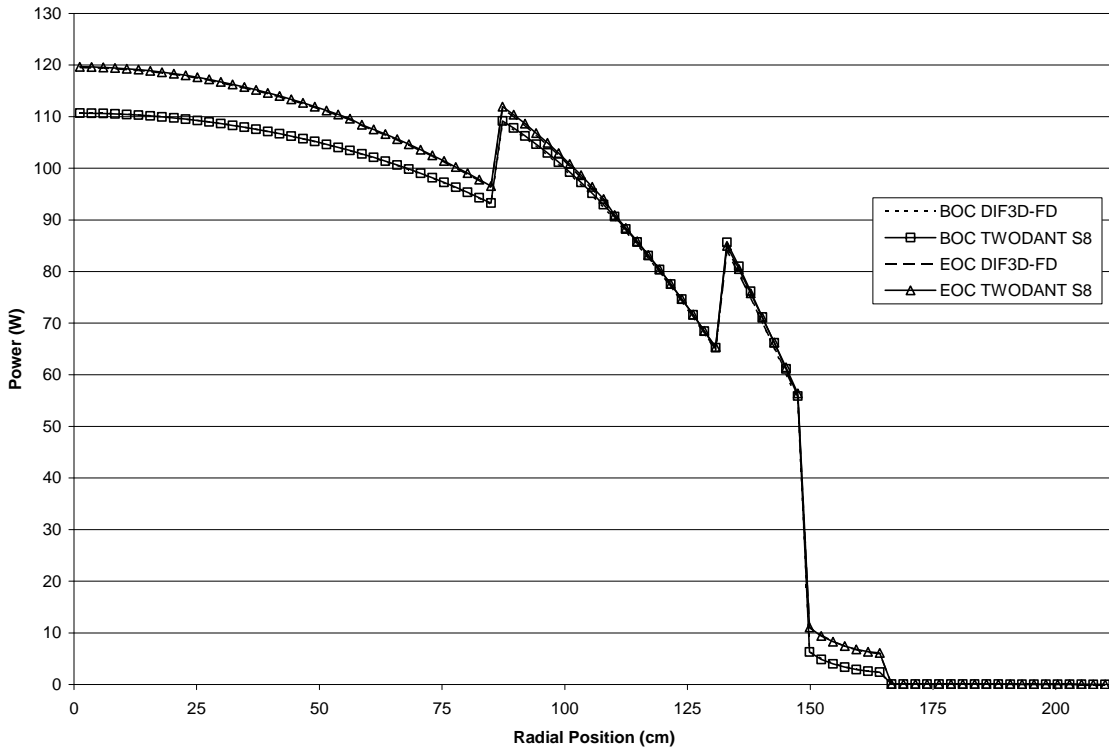


Figure 2.D. Radial Power Plot 45 cm above Core Midplane.

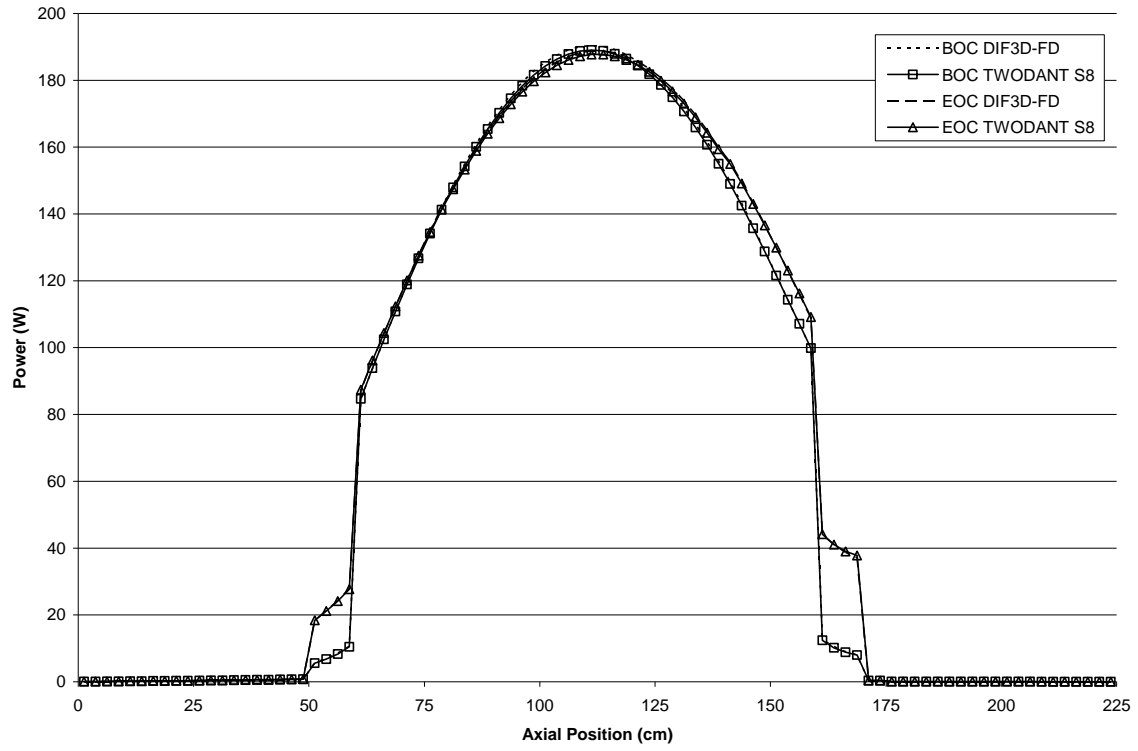


Figure 2.E. Axial Power Plot at Core Centerline.

Table. 3.2 keff by time step (Mode.3)

Mode.3			
k _{eff} Evolution for 900MW, 6 Cycle			
day	Codes		
	REBUS-3 TWODANT S8	Day	REBUS-3 Equilibrium
0	0.99848	0	1.00519
300	1.00323	300	1.00665
360	1.00193		
660	1.00549		
720	1.00385		
1020	1.00648		
1080	1.00468		
1380	1.00663		
1440	1.00481		
1740	1.00626		
1800	1.00449		
2100	1.00558		

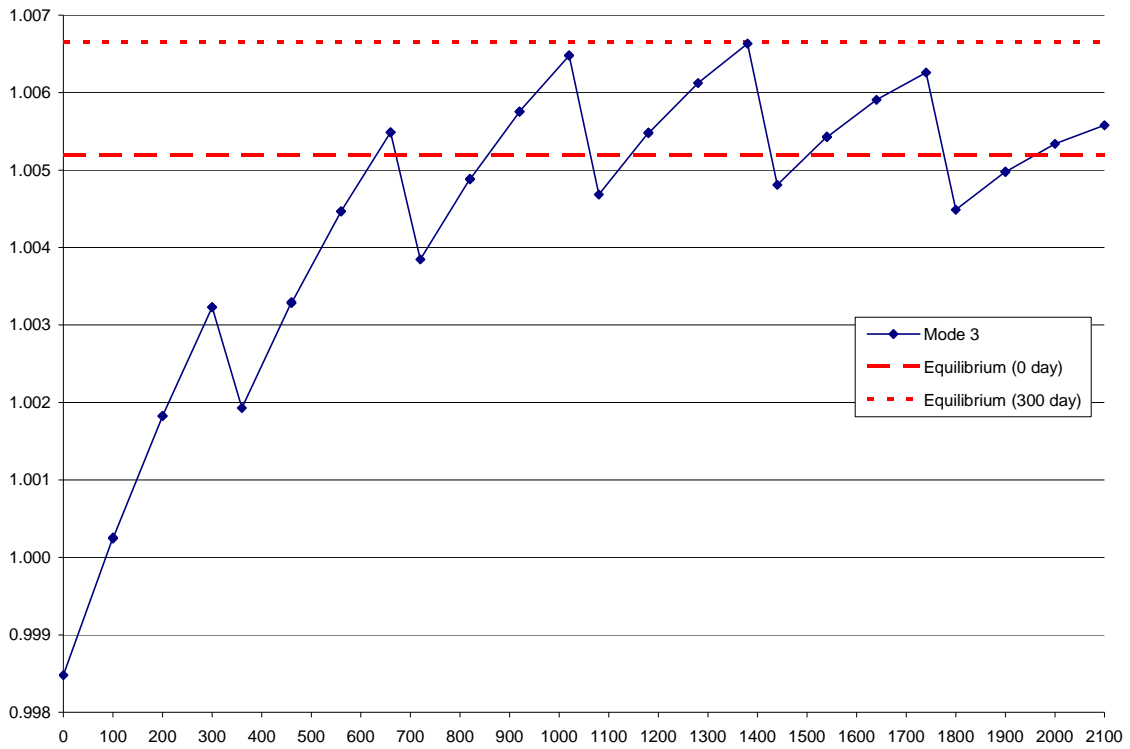


Figure. 3.A plot (Mode.3)

Table. 3.3 Region powers and power peaking factors (Mode.3)

Mode.3					
Time Days	ZONE	Power(Watts)	Power Density (Watts/cc)	Peak Density (Watts/cc)	Peak to AVG. Power Density
0	Core.1	331443000	142	189	1.3
	Core.2	397293000	127	194	1.5
	Core.3	150081000	101	159	1.6
300	Core.1	332682000	143	191	1.3
	Core.2	389925000	125	191	1.5
	Core.3	146328000	99	153	1.6
360	Core.1	332466000	143	191	1.3
	Core.2	391139000	125	191	1.5
	Core.3	146951000	99	154	1.6
660	Core.1	331924000	142	191	1.3
	Core.2	385031000	123	188	1.5
	Core.3	144309000	97	150	1.5
720	Core.1	331854000	142	190	1.3
	Core.2	387048000	124	189	1.5
	Core.3	145254000	98	152	1.5
1020	Core.1	330017000	141	189	1.3
	Core.2	381809000	122	186	1.5
	Core.3	143402000	97	149	1.5
1080	Core.1	330274000	142	189	1.3
	Core.2	384361000	123	187	1.5
	Core.3	144494000	98	150	1.5
1380	Core.1	327532000	140	186	1.3
	Core.2	379705000	121	184	1.5
	Core.3	143198000	97	148	1.5
1440	Core.1	328206000	141	187	1.3
	Core.2	382614000	122	186	1.5
	Core.3	144327000	97	149	1.5
1740	Core.1	324849000	139	184	1.3
	Core.2	378340000	121	182	1.5
	Core.3	143415000	97	147	1.5
1800	Core.1	325971000	140	185	1.3
	Core.2	381489000	122	184	1.5
	Core.3	144514000	98	149	1.5
2100	Core.1	322205000	138	181	1.3
	Core.2	377458000	121	181	1.5
	Core.3	143867000	97	147	1.5

Table. 3.4 Volume averaged neutron spectra in the core (Mode.3)

Mode.3									
day	0			300			360		
Upper group bound. Energy	Core.1	Core.2	Core.3	Core.1	Core.2	Core.3	Core.1	Core.2	Core.3
1.4191E+07	4.9722E+17	5.8139E+17	1.9870E+17	4.9732E+17	5.6843E+17	1.9360E+17	4.9753E+17	5.7084E+17	1.9454E+17
1.0000E+07	8.7784E+18	1.0275E+19	3.4483E+18	8.7802E+18	1.0046E+19	3.3600E+18	8.7839E+18	1.0088E+19	3.3763E+18
6.0653E+06	4.2280E+19	4.9255E+19	1.6202E+19	4.2282E+19	4.8148E+19	1.5787E+19	4.2301E+19	4.8354E+19	1.5863E+19
3.6788E+06	1.1531E+20	1.2934E+20	4.0681E+19	1.1540E+20	1.2653E+20	3.9677E+19	1.1544E+20	1.2705E+20	3.9864E+19
2.2500E+06	2.3804E+20	2.5591E+20	7.2074E+19	2.3870E+20	2.5089E+20	7.0465E+19	2.3870E+20	2.5183E+20	7.0766E+19
1.3647E+06	3.9964E+20	4.2020E+20	1.2007E+20	4.0025E+20	4.1193E+20	1.1750E+20	4.0033E+20	4.1348E+20	1.1799E+20
8.3465E+05	6.6113E+20	6.8701E+20	2.0207E+20	6.6021E+20	6.7273E+20	1.9778E+20	6.6066E+20	6.7541E+20	1.9860E+20
5.1047E+05	8.0049E+20	8.2729E+20	2.4239E+20	7.9910E+20	8.1062E+20	2.3751E+20	7.9972E+20	8.1379E+20	2.3845E+20
3.0962E+05	8.1538E+20	8.3207E+20	2.4038E+20	8.1454E+20	8.1643E+20	2.3584E+20	8.1509E+20	8.1945E+20	2.3673E+20
1.8779E+05	7.3310E+20	7.4429E+20	2.0807E+20	7.3204E+20	7.3059E+20	2.0423E+20	7.3259E+20	7.3325E+20	2.0498E+20
1.1486E+05	5.9962E+20	6.0734E+20	1.6471E+20	5.9773E+20	5.9574E+20	1.6159E+20	5.9836E+20	5.9799E+20	1.6221E+20
6.9663E+04	5.8997E+20	5.8759E+20	1.6118E+20	5.8683E+20	5.7584E+20	1.5799E+20	5.8767E+20	5.7812E+20	1.5862E+20
4.2253E+04	3.6205E+20	3.5781E+20	8.8467E+19	3.5955E+20	3.5038E+20	8.6661E+19	3.6017E+20	3.5181E+20	8.7015E+19
2.5842E+04	4.3618E+20	4.1837E+20	1.0770E+20	4.3219E+20	4.0930E+20	1.0538E+20	4.3310E+20	4.1105E+20	1.0584E+20
1.5674E+04	2.6183E+20	2.4266E+20	5.1821E+19	2.5883E+20	2.3710E+20	5.0655E+19	2.5948E+20	2.3817E+20	5.0882E+19
9.5864E+03	1.4266E+20	1.2824E+20	2.3858E+19	1.4068E+20	1.2513E+20	2.3293E+19	1.4110E+20	1.2572E+20	2.3402E+19
5.8631E+03	1.1760E+20	1.0291E+20	1.9717E+19	1.1548E+20	1.0014E+20	1.9193E+19	1.1590E+20	1.0066E+20	1.9293E+19
3.5561E+03	6.8062E+19	5.7474E+19	9.9598E+18	6.6499E+19	5.5737E+19	9.6615E+18	6.6800E+19	5.6061E+19	9.7177E+18
2.1569E+03	3.7400E+19	3.0190E+19	5.1210E+18	3.6301E+19	2.9144E+19	4.9428E+18	3.6506E+19	2.9336E+19	4.9758E+18
1.3192E+03	1.5593E+19	1.2151E+19	1.9220E+18	1.5036E+19	1.1675E+19	1.8447E+18	1.5138E+19	1.1762E+19	1.8587E+18
8.0012E+02	7.5634E+18	5.8392E+18	9.8114E+17	7.1703E+18	5.5381E+18	9.2696E+17	7.2390E+18	5.5911E+18	9.3642E+17
4.8530E+02	2.1615E+18	1.6253E+18	3.1231E+17	2.0219E+18	1.5260E+18	2.9194E+17	2.0459E+18	1.5432E+18	2.9545E+17
3.2803E+02	1.2905E+18	9.4879E+17	2.5600E+17	1.1621E+18	8.6516E+17	2.3098E+17	1.1833E+18	8.7919E+17	2.3512E+17
1.6020E+02	1.9349E+17	1.4052E+17	6.6979E+16	1.6468E+17	1.2267E+17	5.8276E+16	1.6920E+17	1.2553E+17	5.9666E+16
9.9627E+01	4.7173E+16	3.5085E+16	2.3569E+16	3.6558E+16	2.8458E+16	1.9200E+16	3.8118E+16	2.9462E+16	1.9868E+16
7.4423E+01	3.5575E+16	2.7363E+16	2.3685E+16	2.4972E+16	2.0534E+16	1.8105E+16	2.6442E+16	2.1519E+16	1.8925E+16
4.4025E+01	1.2393E+16	9.8496E+15	9.2105E+15	8.9118E+15	7.5197E+15	7.0906E+15	9.3969E+15	7.8575E+15	7.4043E+15
2.4981E+01	2.2155E+15	1.7496E+15	1.1151E+15	1.5973E+15	1.3402E+15	8.5799E+14	1.6833E+15	1.3995E+15	8.9601E+14
1.5278E+01	2.1584E+15	1.6960E+15	1.2186E+15	1.0411E+15	9.3775E+14	6.9293E+14	1.1651E+15	1.0290E+15	7.5805E+14
9.3443E+00	4.9126E+14	3.8512E+14	2.2241E+14	2.5121E+14	2.2145E+14	1.2686E+14	2.7819E+14	2.4153E+14	1.3860E+14
4.5257E+00	2.5921E+15	2.3023E+15	2.5873E+15	1.6491E+15	1.6655E+15	1.9987E+15	1.7689E+15	1.7524E+15	2.0833E+15
6.1248E-01	1.3947E+14	1.1680E+14	1.1720E+14	6.8474E+13	6.7188E+13	7.4139E+13	7.6067E+13	7.2879E+13	7.9280E+13
4.7304E-01	2.2800E+14	1.8428E+14	1.1391E+14	4.1102E+13	4.5503E+13	3.5933E+13	5.2076E+13	5.5400E+13	4.2349E+13

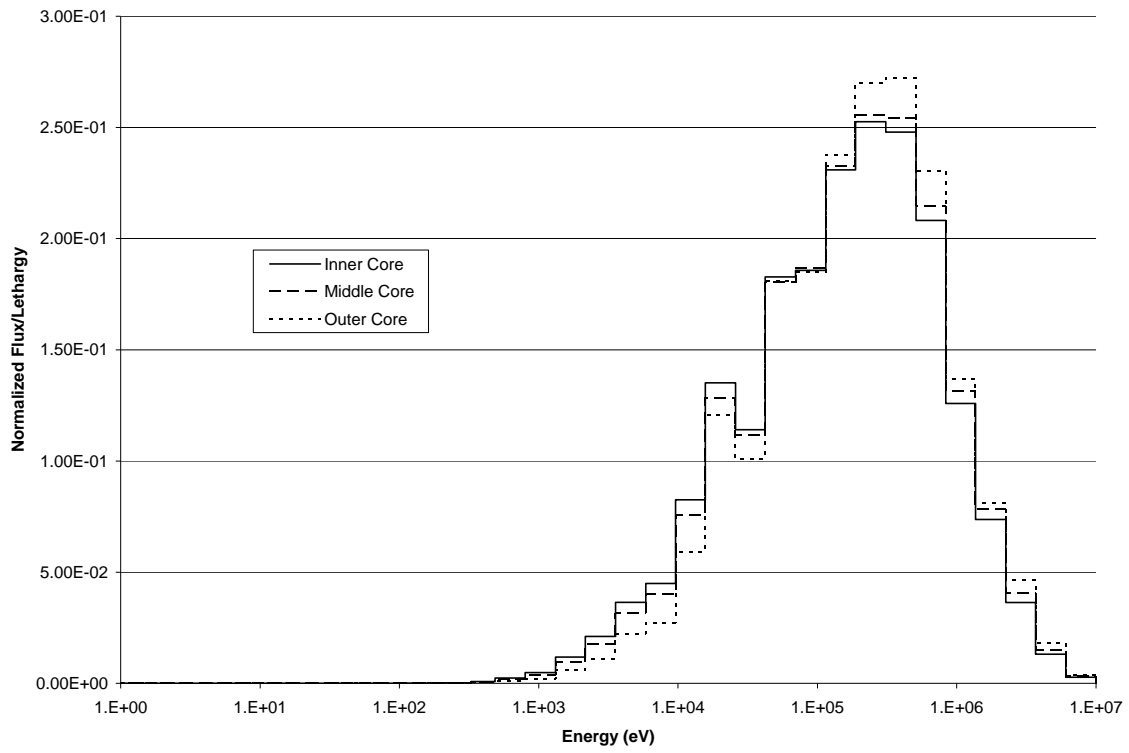


Figure 3.B. Normalized Flux at 0 days.

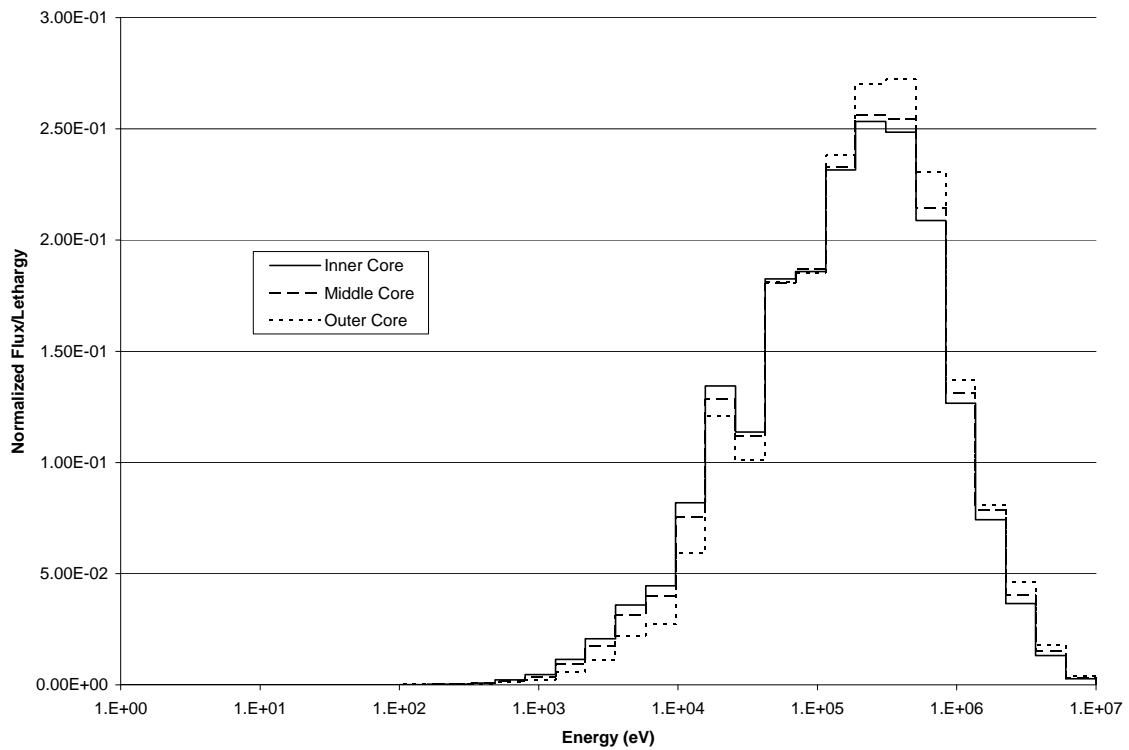


Figure 3.C. Normalized Flux at 300 days.

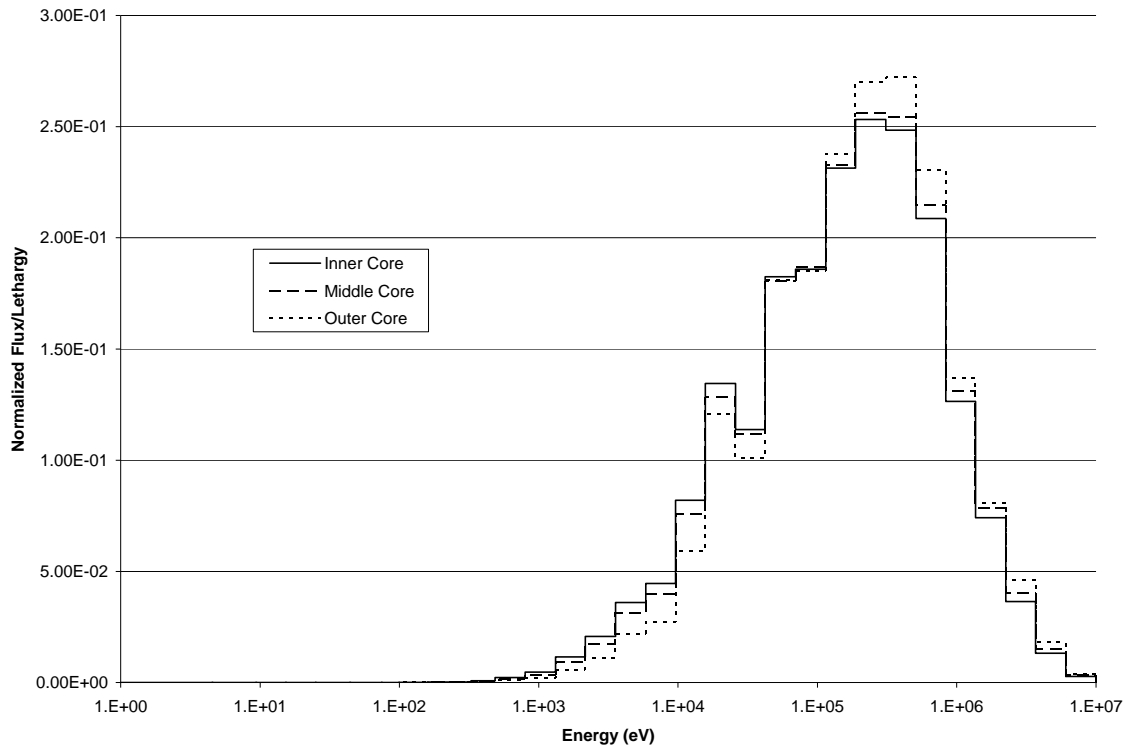


Figure 3.D. Normalized Flux at 360 days.

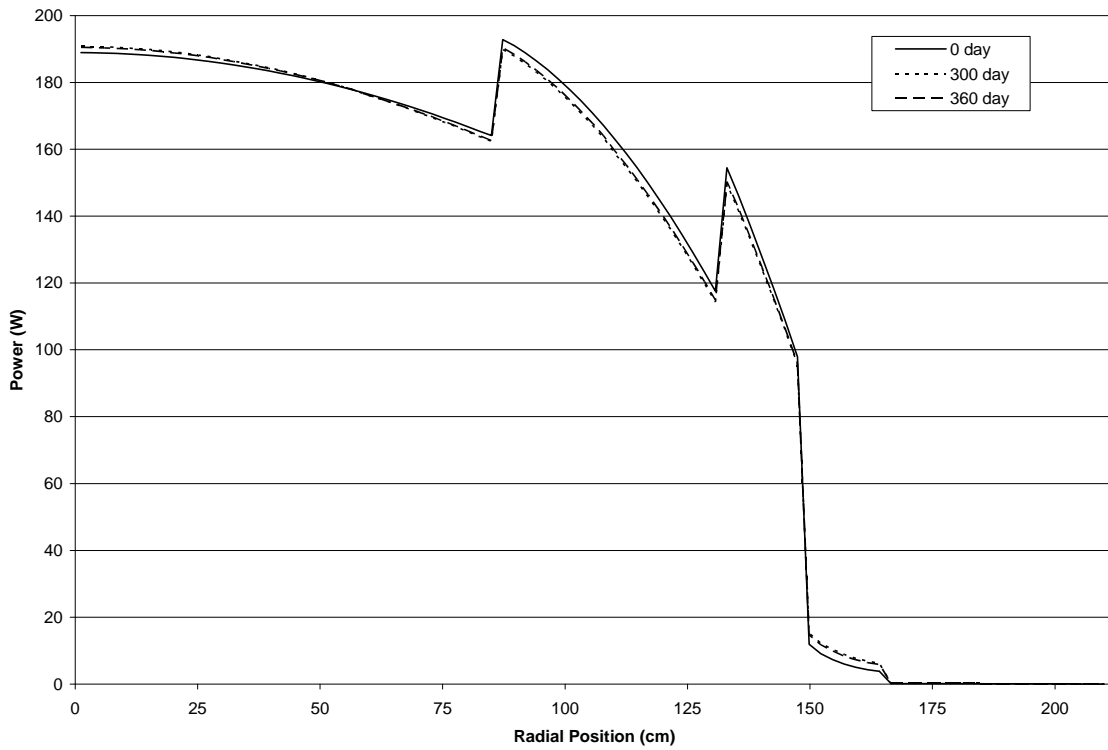


Figure 3.E. Radial Power Plot at Core Midplane.

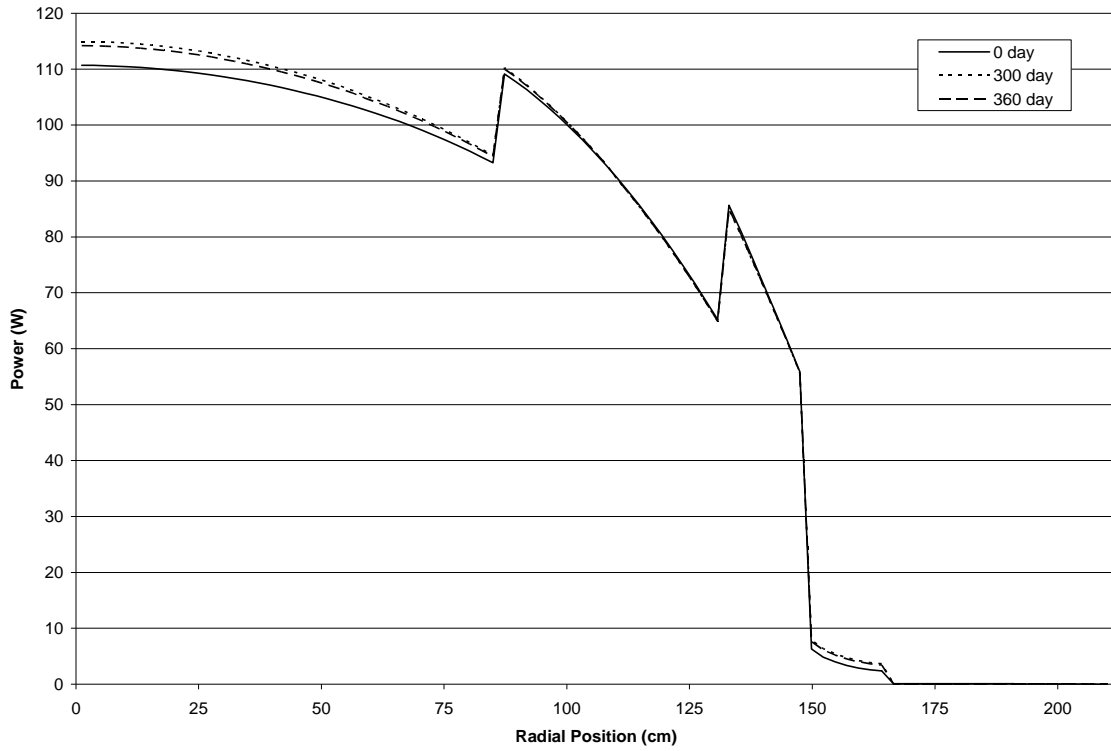


Figure 3.F. Radial Power Plot 45 cm above Core Midplane.

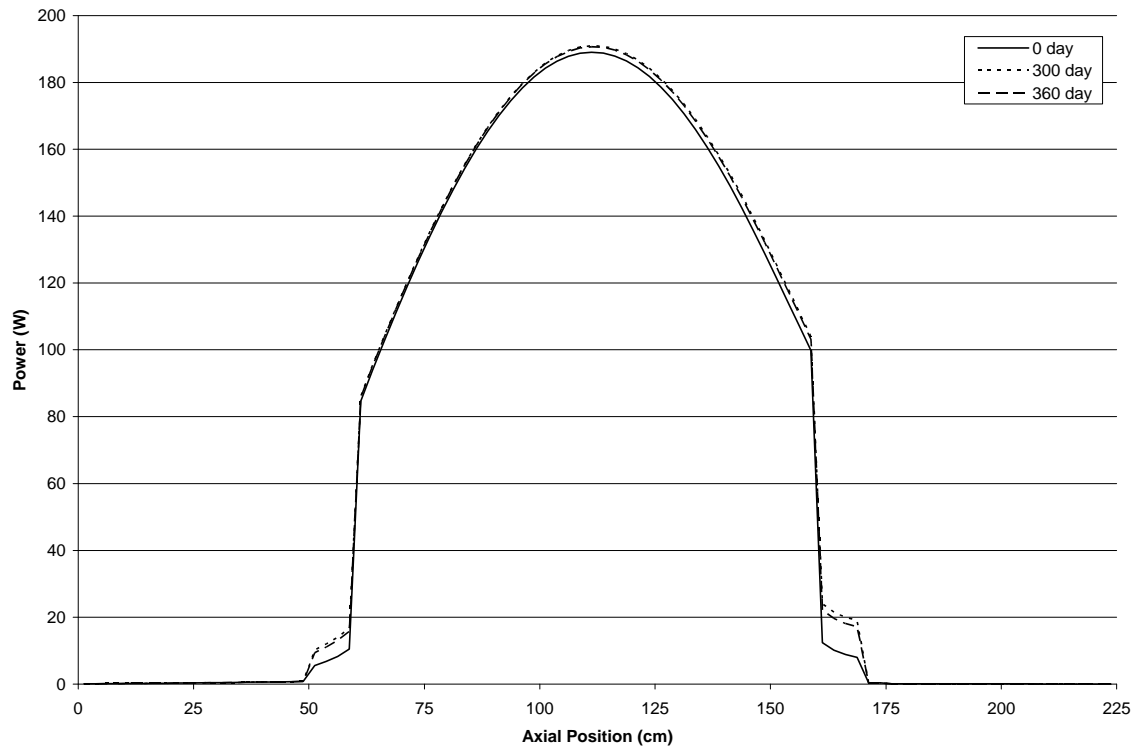


Figure 3.G. Axial Power Plot at Core Centerline.